Physica D 57 (1992) 311–329
North-Holland

PHYSICA D

On the interface dynamics for convection in porous media

Thierry Dombre[1], Alain Pumir[2] and Eric D. Siggia
Laboratory of Atomic and Solid State Physics, Cornell University, Ithaca, NY 14853-2501, USA

Received 19 November 1991
Accepted 11 March 1992
Communicated by J. Guckenheimer

We study analytically the problem of convection in two-dimensional porous media, in the limit where a sharp interface develops between the hot and cold fluids. We propose a first approximation which is found to be "pole conserving" and displays a rather smooth dynamics with an asymptotic growth of the interface width linear in time. We then reconsider the initial value problem and solve it exactly at short times. A new nonlocal mechanism is pointed out, by which algebraic singularities and critical points of the map describing the interface shape may proliferate. Prospects for further work are discussed in the conclusion.

1. Introduction

Convection in two-dimensional porous media has received until now much less attention than the relation problem of viscous fingering in a Hele Shaw cell (for reviews see ref. [1])[#1]. However, from a theoretical point of view, it can be seen as the minimal model in fluid mechanics incorporating both advection and incompressibility, two ingredients at the heart of Euler's equations. Indeed, in the absence of any viscosity or thermal diffusivity effects, the problem describes the advecation of an active scalar θ (a properly nondimensionalized temperature variable)

$$\frac{\partial \theta}{\partial t} + \boldsymbol{v} \cdot \nabla \theta = 0 , \tag{1.1}$$

in a two-dimensional incompressible velocity field

$$\boldsymbol{v} = \theta \hat{\boldsymbol{y}} - \nabla \phi , \qquad \nabla \cdot \boldsymbol{v} = 0 . \tag{1.2}$$

Without the gradient (or pressure term) in the definition of the velocity, (1) and (2) are nothing but the 2D-inviscid Burgers equation which is known to develop shocks in finite time. Here the physics is seriously complicated by the incompressibility constraint.

Recently two of us [3] have solved (1.2) numerically for θ initially a smooth function of space. In certain regions, the contour lines of θ bunch together such that the thickness of the "interface" thus formed remains smaller than, but of order of, the radius of curvature of an individual line. Of course the area between any two contour lines of θ is constant so that if they

[1] Permanent address: CRTBT-CNRS 25, Avenue des Martyrs, B.P. 166, 38042 Grenoble Cedex 09, France.
[2] Permanent address: Laboratoire de Physique Statistique, Ecole Normale Supérieure, 24 rue Lhomond, 75231 Paris Cedex 05, France.
[#1] Hele Shaw flows with two fluids of different density and same viscosity, a situation very close to ours in the limit of a very sharp interface, were studied numerically by G. Tryggvasson and H. Aref [2], however with a nonzero interface tension. While completing the writing of this paper, we became aware of a recent convection experiment done by P. Tabeling and G. Zocchi at the Ecole Normale Superieure (Paris) and theoretical work by M. Ben Amar (private communication).

0921-4526/92/$05.00 © 1992 – Elsevier Science Publishers B.V. All rights reserved

pinch together in one region, they must either elongate or balloon out elsewhere. Define the center of the interface by where $|\nabla\theta|$ has a local maximum for fixed x. The interface continues to thin and fold leading to a finite time divergence in the global maximum of $|\nabla\theta| \sim 1/(t^* - t)$. In the vicinity of where $|\nabla\theta|$ is maximum, the interface never develops noticeable overhangs as would occur for Kelvin–Helmholtz rollup. The radius of curvature always remains larger than but of order of the thickness. The "jump" in θ across the interface remains nearly constant in time, but its shape varies considerably and roughly periodically as a function of $-\ln(t^* - t)$.

The differential statement of area preservation implies that the local stretching diverges like the inverse thickness, $|\nabla\theta|$, or curvature. Although the numerics can only follow the collapse at one point, it is clear that an infinity of points along the interface become singular all more or less independently.

Motivated by these findings, we decided to study the problem analytically in more detail. When the thickness of the interface is small compared to its radius of curvature, one may consider that the vorticity $\boldsymbol{\omega} = \nabla \times \boldsymbol{v} = \partial_x \theta \hat{z}$ is concentrated on a line with a density per unit length equal to $\sin\alpha$ where α is the angle between the local tangent to the interface and the horizontal and the jump in θ across the interface is scaled to one. The Biot–Savart law then gives the following equation for the evolution of the interface,

$$\partial_t \bar{z}(\gamma, t) = \frac{1}{2\pi \mathrm{i}} \,\mathrm{PV} \int_{-\infty}^{+\infty} \frac{(\partial y/\partial\gamma)(\gamma', t)\,\mathrm{d}\gamma'}{z(\gamma, t) - z(\gamma', t)}\,, \tag{1.3}$$

in which $z = x + \mathrm{i}y$ is the complex position of the interface ($\bar{z}$ its complex conjugate), γ is a Lagrangian variable and the integral is a principal value integral. Equation (1.3) is the starting point for the analysis carried out in this paper, and no further use of eq. (1.1) and (1.2) is made.

The relation between the singularities of (1.3) and (1.1), (1.2) is far from evident. For instance, according to (1.3) the spectrum of linearized modes for the straight interface amplify at a rate proportional to wavenumber with no short distance cutoff such as would be supplied by the interface thickness. It is not even evident that (1.3) errs in the direction of enhancing the blow up, since some spurious singularity that leaves $|\partial_\gamma z|$ bounded (n.b. the stretching diverged for (1.1), (1.2)) could intervene and limit the times for which (1.3) is a sensible model of (1.1), (1.2). Presumably if the solutions of (1.3) remain smooth, then they will agree with (1.1), (1.2) with suitable initial conditions, for some period of time. Less obviously, a solution to (1.3) for which the cumulative stretching exceeds the curvature may be promoted into a solution of (1.1), (1.2) since at least the premises on which (1.3) was derived remain valid.

Unfortunately, we see no way of ascertaining the behavior of (1.3) short of actually solving it. This is an exercise of some interest because (1.3) is nonlocal and it is the presence of a solution to the Poisson equation, ϕ, in (1.2) which makes the continuous problem more complex than a simple hyperbolic system. There is no obvious way to "localize" (1.3) when the distortions of the interface are large.

In section 2 we approximate the denominator by the first term in its Taylor expansion which turns (1.3) into a Hilbert transform: still nonlocal but more tractable. The tangential discontinuity of the velocity is also preserved. Using x and t rather than γ and t as independent variables, we show that this approximation leads to a pole conserving dynamics where meromorphic initial conditions remain meromorphic at all time. Since the interface remains smooth, whereas solutions to (1.1), (1.2) do not, we tend to believe that the approximation is in error.

In section 3 we solve exactly the initial value problem at small times and find that eq. (1.3) may generate an infinite number of singularities and zeros of the derivative maps $\partial_x z$ or $\partial_x \bar{z}$, even

for simple meromorphic initial conditions. The nonlocal mechanism we shall point out is rather unusual for hyperbolic systems and might be considered as an intrinsic source of chaos missed by our first approximation. The appendix illustrates, in the particular case of a cubic shape of the interface at the initial time, the mathematical notions we are forced to introduce and manipulate in section 3. Finally the conclusion summarizes the unanswered questions which should be addressed in the future.

2. A pole conserving approximation

In order to remove the weight, $(\partial y/\partial\gamma)(\gamma, t)$, in the numerator of the integral in eq. (1.3), it would be tempting to parameterize the interface by y rather than with a Lagrangian variable γ. However, as soon as the interface is folded, z is not a single-valued function of y anymore, which makes the choice of this parameterization of little interest to study a folding instability. The choice of x as an independent variable is more reasonable since overhangs were not observed numerically and it is selfconsistent to assume that z is a function of x at later times if it is so initially. Of course, this can only be asserted within our approximations and for a limited period of time. We rewrite the equation of motion as (an overbar denotes complex conjugation),

$$\partial_t \bar{z}(\gamma, t) = -\frac{1}{2\pi}\,\mathrm{PV}\int_{-\infty}^{+\infty} \frac{\mathrm{d}z}{z(\gamma, t) - z(\gamma', t)} + \frac{1}{2\pi}\,\mathrm{PV}\int_{-\infty}^{+\infty} \frac{(\partial x/\partial\gamma)(\gamma', t)\,\mathrm{d}\gamma'}{z(\gamma, t) - z(\gamma', t)}\,, \tag{2.1}$$

where $\mathrm{d}z$ is a short notation for $(\partial z/\partial\gamma)(\gamma', t)\,\mathrm{d}\gamma'$. The first term in the right hand side of (2.1) is integrated exactly as

$$+\frac{1}{2\pi}\log\left(\frac{z(\infty, t) - z(\gamma, t)}{z(\gamma^+, t) - z(\gamma, t)}\,\frac{z(\gamma^-, t) - z(\gamma, t)}{z(-\infty, t) - z(\gamma, t)}\right). \tag{2.2}$$

Provided $z(\pm\infty, t)$ are both infinite with a well-defined limiting argument, the expression above is independent of γ and equal to

$$\frac{1}{2\pi}\left[\mathrm{Arg}\, z(\infty, t) - \mathrm{Arg}\, z(-\infty, t) \pm \pi\right]. \tag{2.3}$$

The sign of π inside the brackets of (2.3) is entirely determined by the requirement that the whole quantity be between $-\pi$ and π. Therefore we get zero for an asymptotically flat interface or a cubic like curve and $\frac{1}{2}\mathrm{i}\,\mathrm{sgn}(\rho)$ for the parabola $y = x^2/2\rho$. In any case, this boundary term just gives rise to a uniform velocity along the vertical direction which does not affect the shape of the interface and we shall ignore it in the following.

We now have

$$\mathrm{d}_t \bar{z}(x, t)|_\gamma = \frac{1}{2\pi}\,\mathrm{PV}\int \frac{\mathrm{d}x'}{z(x, t) - z(x', t)} = \mathrm{i}g(x, t)\,, \tag{2.4}$$

where the left hand side is the Lagrangian velocity, (d_t is a total time derivative at fixed γ), and the last equality defines $g(x, t)$. Henceforth, z will be a function of x and t. But

$$\mathrm{d}_t \bar{z}(x, t)|_\gamma = \partial_t \bar{z}(x, t) + \mathrm{d}_t x|_\gamma\, \partial_x \bar{z}(x, t)\,, \tag{2.5}$$

whence follows, since $\partial_x \bar{z} + \partial_x z = 2$,

$$\partial_t \bar{z}(x, t) = \tfrac{1}{2}(\mathrm{d}_t \bar{z}(x, t)|_\gamma\, \partial_x z(x, t) - \mathrm{d}_t z(x, t)|_\gamma\, \partial_x \bar{z}(x, t))\,. \tag{2.6}$$

Using (2.4) and the complex conjugate equation $\mathrm{d}_t z = -\mathrm{i}\bar{g}$ we finally obtain

$$\partial_t y(x, t) = \frac{1}{2\mathrm{i}}\,\partial_t(z - \bar{z}) = -\tfrac{1}{2}(g\partial_x z + \bar{g}\partial_x \bar{z})\,. \tag{2.7}$$

Until now the series of transformations leading from (2.1) to (2.7) were exact, though not obviously useful. We now propose an approximate treatment of (2.7) where the denominator entering the definition of $g(x, t)$, $z(x, t) - z(x', t)$, is simply replaced by the first term of its Taylor expansion, $\partial_x z(x', t)(x - x')$. Note that this assumption leaves some nonlocal features in the problem. It was previously used by Caflisch and Semmes [4] for the Kelvin Helmholtz instability as the first step in their reduction of the Birkhoff–Rott integral to a nonlinear wave equation. They were able to justify this approximation for the isolated curvature singularities they were interested in, which did not involve strong distortions of the vortex sheet. The singularities pertinent here are stronger, as already noted in the introduction, and our assumption is merely an uncontrolled first approximation. Quite amusingly, we shall find a pole conserving dynamics, some what reminiscent of the one known to govern the Saffman–Taylor instability without surface tension [5]. It should be emphasized, however, that in the latter problem conformal mapping techniques can be used and that the resulting dynamical equations for conformal singularities are exact.

As announced in the last paragraph, we replace in (2.7) g and $\bar{g}$ by the Hilbert transforms of $-1/\partial_x z$ and $+1/\partial_x \bar{z}$, respectively. Differentiating (2.7) once with respect to x, allows one to close the equation for $\partial_x z$ or $\partial_x \bar{z}$ as

$$\frac{1}{2\mathrm{i}}\,\partial_t(\partial_x z - \partial_x \bar{z}) = \tfrac{1}{2}\partial_x\left(H\left(\frac{1}{\partial_x z}\right)\partial_x z - H\left(\frac{1}{\partial_x \bar{z}}\right)\partial_x \bar{z}\right). \tag{2.8}$$

Let $(\partial y/\partial x)(x)$ be a rational function of the form (P/Q) where P and Q are two real polynomials in x of degree m and n. Then $P - \mathrm{i}Q$ and $P + \mathrm{i}Q$ are two polynomials of degree $p = \sup(m, n)$ which can be parametrized as

$$P - \mathrm{i}Q = a_0 \prod_{i=1}^{p} (x - a_i)\,,$$

$$P + \mathrm{i}Q = \bar{a}_0 \prod_{i=1}^{p} (x - \bar{a}_i)\,. \tag{2.9}$$

For this restricted class of mappings, the geometry of the interface is entirely specified by the positions of the p zeros of $P - \mathrm{i}Q$ and the phase of a_0, while the amplitude of a_0 disappears in the ratio P/Q. For $m > n$, a_0 is real and imaginary for $n > m$; its phase is arbitrary when $m = n$. Zeros of $P - \mathrm{i}Q$ and $P + \mathrm{i}Q$ are poles of $1/\partial_x z$ and $1/\partial_x \bar{z}$, respectively, and the exact computation of $H(1/\partial_x z)$ and $H(1/\partial_x \bar{z})$ in the r.h.s. of (2.8) is straightforward. One obtains

$$\partial_t\left(\frac{P}{Q}\right) = -\tfrac{1}{4}\partial_x\left(\frac{R}{Q}\right), \tag{2.10}$$

where R is a polynomial in x of degree not greater than $p - 1$ given by

$$R = (P - \mathrm{i}Q) \times \left(\sum_{i=1}^{p} \epsilon_i \frac{Q(a_i)}{P'(a_i) - \mathrm{i}Q'(a_i)} \frac{1}{x - a_i}\right) + \text{c.c.} \tag{2.11}$$

with $\epsilon_i = \mathrm{sgn}(\mathrm{Im}\, a_i)$. We ignore the nongeneric case where $P + \mathrm{i}Q$ has a double zero. In the following we shall denote

$$\beta_i = \frac{Q(a_i)}{P'(a_i) - \mathrm{i}Q'(a_i)}\,, \tag{2.12}$$

which is nothing but the residue of the map $\mathrm{i}/\partial_x z$ at the pole a_i.

Integrating (2.10) along a closed contour, which does not contain any new zeroes of Q, one can easily show that the residues of P/Q are constants of the motion. As a consequence, no new zero of Q can appear as a function of time, and thus, the degree of Q (and therefore the number of poles of $\partial_x z$ or $\partial_x z^*$) is conserved. On the other hand the degree of P determines the behavior of the interface at the infinity. Letting x go to infinity in (2.10), we find that m does not vary unless $m < p - 2$. We conclude that n and p are preserved by the dynamics and it suffices to

establish now the equations of motion of the zeros a_i and the phase of a_0. Multiplying both sides of (2.10) by Q^2 we get

$$\frac{1}{2\mathrm{i}}\left[(P-\mathrm{i}Q)\,\partial_t(P+\mathrm{i}Q)-(P+\mathrm{i}Q)\,\partial_t(P-\mathrm{i}Q)\right] = \tfrac{1}{4}\left[Q\partial_x R - R\partial_x Q\right]. \tag{2.13}$$

The absence of the monomial x^{2p} and x^{2p-1} on the r.h.s. of (2.13) implies

$$\mathrm{d}_t(\bar{a}_0/a_0)=0\,, \tag{2.14a}$$

$$\mathrm{d}_t\sum_{i=1}^{p}(a_i-\bar{a}_i)=0\,, \tag{2.14b}$$

which shows that a_0 is a constant of motion (its magnitude does not enter P/Q), as is the imaginary part of the "center of mass" of the a_i. Much more algebra is required to find the dynamics of each a_i. We indicated here a few intermediate steps in the computation and quote the final result. Dividing both sides of (2.13) by $P-\mathrm{i}Q$ and equating the residues of the pole a_i, one obtains

$$\mathrm{d}_t a_i = \tfrac{1}{4}\left\{\frac{1}{a_0\prod_{j\neq i}(a_i-a_j)}\times\left[R'(a_i)-R(a_i)\left(\sum_k\frac{1}{a_i-\bar{a}_k}\right)\right]+\frac{R(a_i)}{\bar{a}_0\prod_k(a_i-\bar{a}_k)}\right\}. \tag{2.15}$$

Equation (2.11) yields

$$R(a_i)=\epsilon_i\beta_i a_0\prod_{j\neq i}(a_i-a_j)+\sum_k\epsilon_k\bar{\beta}_k\frac{P(a_i)+\mathrm{i}Q(a_i)}{a_i-\bar{a}_k}\,, \tag{2.16}$$

and upon differentiation with respect to x,

$$R'(a_i)=\sum_{j\neq i}(\epsilon_i\beta_i+\epsilon_j\beta_j)a_0\prod_{k\neq i,j}(a_i-a_k)+\sum_k\epsilon_k\bar{\beta}_k\frac{P(a_i)+\mathrm{i}Q(a_i)}{a_i-\bar{a}_i}\times\left(\sum_j\frac{1}{a_i-\bar{a}_j}-\frac{1}{a_i-\bar{a}_k}\right). \tag{2.17}$$

Inserting (2.16) and (2.17) into (2.15) one is led after some straight-forward algebraic manipulations to the equation

$$\mathrm{d}_t a_i=\tfrac{1}{4}\sum_{j\neq i}(\epsilon_i\beta_i+\epsilon_j\beta_j)\frac{1}{a_i-a_j}+\frac{1}{8\mathrm{i}}\epsilon_i+\tfrac{1}{4}\sum_j\frac{1}{a_i-\bar{a}_j}\left(\epsilon_j\bar{\beta}_j-\epsilon_i\beta_i-2\mathrm{i}\frac{\epsilon_j\bar{\beta}_j\beta_i}{a_i-\bar{a}_j}\right), \tag{2.18}$$

where it should be understood from the definition (2.12) that the β_j are entirely determined by the a_j according to the formula

$$\beta_j=\frac{1}{2\mathrm{i}}\frac{\prod_k(a_j-\bar{a}_k)\bar{a}_0}{\prod_{k\neq j}(a_j-a_k)a_0}\,. \tag{2.19}$$

As in the Saffman–Taylor problem the nonlinear and nonlocal evolution equation (2.8) has been reduced to a set of ordinary differential equations (2.18) for the dynamics of zeros of the map $\partial_x z$. In the former case, it is known that zeros of the derivative map can hit the physical axis in finite time, corresponding in that case to the formation of a cusped interface [5]. We do not find such events here, at least for simple enough initial conditions. In fact eq. (2.18) does not allow a zero to reach the real axis in finite time while remaining beyond some nonzero distance from the others. Indeed for an isolated zero a_i, close to the real axis, (2.19) gives $\beta_i\sim \mathrm{e}^{\mathrm{i}\varphi}(a_i-\bar{a}_i)$ to leading order in the small quantity $(a_i-\bar{a}_i)$ and one gets from (2.18)

$$\mathrm{d}_t a_i=\tfrac{1}{4}\sum_{j\neq i}\left(\frac{\epsilon_j\beta_j}{a_i-a_j}+\text{c.c.}\right)-\frac{\epsilon_i}{4}\sin\varphi+\mathcal{O}(a_i-\bar{a}_i)\,. \tag{2.20}$$

The terms of order one in the r.h.s. of (2.20) turn out to be real and we conclude that a_i cannot approach the real axis more rapidly than exponentially. The argument breaks down for zeros which approach each other and the real axis together. In any event, rational functions of x will not describe the cusps characteristic of roll up. (Certainly algebraic singularities are required).

The dynamics contained in eq. (2.18), though approximate, may deserve further investigation. We conclude this section by discussing a few examples which illustrate well the physics behind the pole conserving approximation, while lending themselves to easy computation. For all the simple polynomial maps we shall consider, it is more convenient to work directly with eq. (2.10). We start with the parabola $y = x^2/2\rho$; then $P = x/\rho$, $Q = 1$, $P - iQ$ has a single zero at $x = i\rho$ and $R = 2\,\mathrm{sgn}\,\rho$. Therefore, the parabola has a stationary shape and taking into account the boundary term discussed at the beginning of this section, we find that it moves with constant velocity $-\mathrm{sgn}\,\rho$ along the vertical axis. The result is exact and correctly captured by the approximation of this section. In this case the zero of $\partial_x z$ is not moving at all.

Next, we consider the cubic $y = \frac{1}{6}x^3 + cx$; then $P = \frac{1}{2}x^2 + c$, $Q = 1$ and $P - iQ$ has a pair of zeros at $x = \pm x_0 = \pm\sqrt{2(i - c)}$ (these points are also introduced in the appendix). From the definition of R one gets $R = x(1/x_0 + 1/\bar{x}_0)$ which upon insertion in (2.10) leads to

$$d_t c = -\frac{1}{4}\,\frac{\sqrt{-c + \sqrt{1 + c^2}}}{\sqrt{1 + c^2}}\,. \tag{2.21}$$

The slope at the origin, c, is continuously decreasing with t, very slowly at large positive values of c, more rapidly at moderate values of c. A pair of folds appears on the interface for $c < 0$ corresponding to the two roots $\pm x_0$. At large negative values of c, (2.21), simplifies to

$$d_t c = -\tfrac{1}{4}\sqrt{2}\,\frac{1}{\sqrt{|c|}}\,, \tag{2.22}$$

which shows that $|c|$ behaves asymptotically like $t^{2/3}$. This means in turn that the height of the folds grows like t at late times, a sensible result for the convection in porous media. As for the zeros of $\partial_x z$, it can be checked that they first move towards the real axis and then asymptote to it at infinity.

The case of a nearly flat, periodically perturbed interface is particularly revealing. We take $y = \delta \sin kx$ with k, $d > 0$. Then $P = k\delta \cos kx$, $Q = 1$ and the zeros of $P - iQ$ satisfy

$$ka_{\pm n} = \pm\tfrac{1}{2}\pi \mp i\,\mathrm{Arg\,sinh}\left(\frac{1}{\delta k}\right) + 2n\pi\,, \tag{2.23}$$

whence follows the expression of R,

$$R = -\frac{1}{2\sqrt{1 + (\delta k)^2}}\,[\cot\tfrac{1}{2}k(x - a_{+0}) + \cot\tfrac{1}{2}k(x - a_{-0})](P - iQ) + \text{c.c.} \tag{2.24}$$

which simplifies to

$$R = -\frac{2\delta k}{\sqrt{1 + (\delta k)^2}}\sin kx\,. \tag{2.25}$$

Equation (2.10) then yields

$$d_t \delta = \frac{1}{2}\,\frac{\delta k}{\sqrt{1 + (\delta k)^2}}\,. \tag{2.26}$$

The Mullins–Sekerka instability is recovered for small amplitudes with an amplification rate of disturbances scaling like their wave vector. However, the instability saturates for large amplitudes and we find within our approximation that the width of the interface in the y direction grows asymptotically like $\frac{1}{2}t$.

3. Beyond the pole conserving approximation

Within the approximation developed in section 2, meromorphic initial conditions remain meromorphic at later times and as a consequence the number of zeros of $\partial_x z$ and $\partial_x \bar{z}$, i.e. the

critical points of the maps z and $\bar{z}$, is conserved. In the few simple examples we examined, we found that these points, generally far from the real axis ($\mathrm{Im}\, x = 0$), move towards it, initially, though never reach it in finite time. If the scale of $\partial_x y(x, t)$ is large compared to 1, then these critical points are associated with folds of the interface, whose scale along the vertical direction grows like t in the final stages of evolution. This picture of the interface dynamics is a rather smooth one, difficult to reconcile with the numerical observations, which point to a finite time blow up of the interface stretching, preceded by some seemingly chaotic folding [3]. We therefore believe that some qualitative aspects of the problem have been lost in our first treatment and in this section we solve (2.7) more precisely for short times.

Let us consider again the case of a cubic curve at the initial time, $y(x, t=0) = \frac{1}{6}x^3 + cx$. The right-hand side of the equation of motion (2.7) can be calculated exactly, using standard contour deformation techniques. This yields, at $t = 0$,

$$\partial_t y = \tfrac{1}{2}\sqrt{3}\,\mathrm{Im}\left(\frac{x}{\sqrt{x^2 + 8(c - \mathrm{i})}}\right). \tag{3.1}$$

The velocity field has a much richer structure than what was obtained in (2.21), using the pole conserving approximation. The most notable feature of (3.1) is the appearance of inverse square root singularities at $x = \pm 2\sqrt{2(\mathrm{i} - c)} = \pm x_1$ (and at complex conjugate positions). On the other hand the critical points of z are at $x = \pm\sqrt{2(\mathrm{i} - c)} = \pm x_0$ and one quickly realizes that x_0 and x_1 obey the relation $z(\pm x_1) = z(\mp x_0)$. We shall say in the following that x_1 and $-x_0$ are co-preimages under z since they share the same value of z. In the same way $\bar{x}_1$ and $-\bar{x}_0$ are co-preimages under $\bar{z}$.

Equation (3.1) suggests the formation of square root singularities at co-preimages of critical points. This richer analytic structure may in turn contain new critical points in the vicinity of the co-preimages, allowing then the process to repeat. This section is devoted to a thorough analysis of this problem in a general situation. We shall see that the formation of a singularity from smooth initial conditions is described by a local nonlinear equation, which can be solved exactly at short times. The possibility of a cascading process and the overall pattern of singularities which should result from it, depend solely on the initial interface shape. We discuss this last matter in an appendix, in the particular case of the cubic.

3.1 Analytic continuation of the equation of motion

Since we are a priori interested in the dynamics at points x which are not necessarily on the real axis, we first need to analytically continue the function $g(x, t)$ in (2.4). For x on the real axis, $g(x, t)$ is defined as half the integral of the function $1/[z(x, t) - z(x', t)]$ on the two contours displayed in fig. 1. Suppose that we let x move, say, in the upper half complex plane, on

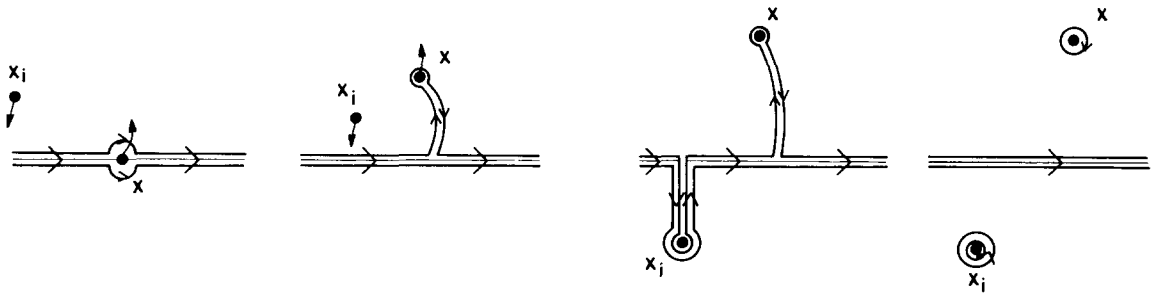

Fig. 1. The various deformations of contours used to derive eq. (3.3).

a path avoiding any singularity of z. The upper contour is deformed in such a way that it still encircles x clockwise, while remaining on the same Riemann sheet as x (i.e. avoiding also any singularity z). The lower contour is left untouched and by using the Cauchy formula to estimate the first contribution, we get the usual analytic continuation of a principal value integral,

$$g(x,t) = \frac{1}{2i\pi}\int_{-\infty}^{+\infty} \frac{dx'}{z(x,t)-z(x',t)} \pm \tfrac{1}{2}\,\frac{1}{\partial_x z(x,t)}\,, \tag{3.2}$$

where the $\pm$ depends on whether x is in the upper or lower half complex plane.

However, more needs to be said. As soon as the interface is not flat anymore, we know that the inverse map is multi-valued. Let ω_i be the ith inverse of z: to each point x we can associate a countable set of co-preimages $x_i = \omega_i(z(x))$. The x_i are functions of x and t but very often we shall drop the two arguments to simplify the notations. Since the x_i move together with x, some of them may cross the real axis either downwards or upwards during the analytic continuation process. Each time this happens, the residue at x_i should be subtracted from or added to the right-hand side of (3.2), in order that the first term in (3.2) is always defined as the integral along the real axis (see again fig. 1 for an intuitive picture).

The final results reads

$$g(x,t) = \frac{1}{2i\pi}\int_{-\infty}^{+\infty} \frac{dx'}{z(x,t)-z(x',t)} \pm \tfrac{1}{2}\,\frac{1}{\partial_x z(x,t)} + \sum_i \pm \frac{1}{\partial_x z(x_i,t)}\,. \tag{3.3}$$

The residue at x_i gets a weight ± 1 because both contours are pushed up or down with x_i. Note that not all x_i obeying $z(x_i) = z(x)$ appear in (3.3) but only those which cross the real axis an odd number of times during the analytic continuation towards x.

Before continuing the evolution equation (2.7) we must clarify the meaning of the "conjugate" to be denoted by "$*$" for functions of complex x. We define, $z^*(x) = x - iy(x) \equiv \overline{z(\bar{x})}$, and similarly for g^*. Clearly this agrees with complex conjugation for x real and allows us to write $\partial_x z + \partial_x z^* = 2$. Therefore (2.7) follows from (2.4) as before with overbars replaced by stars.

The integral expression for g^* is continued to complex x as above. We define the co-preimages of x under z^* as $x_{*i} = \omega_i^*(z^*(x))$ where ω_i^* is the ith branch of the inverse of z^*. Note that the set $\{x_{*i}\}$ is not the complex conjugation of the $\{x_i\}$ unless x is real. An expression analogous to (3.3) is then obtained for $g^*(x,t)$, which leads to the desired analytic continuation of the equation of motion (2.7)

$$\frac{1}{2i}\,\partial_t(z - z^*) = -\frac{1}{4i\pi}\,\partial_x z \int \frac{dx'}{z-z'} + \frac{1}{4i\pi}\,\partial_x z^* \int \frac{dx'}{z^* - z'^*} - \tfrac{1}{2}\sum_i \pm \frac{\partial_x z(x)}{\partial_x z(x_i)} + \tfrac{1}{2}\sum_i \pm \frac{\partial_x z^*(x)}{\partial_x z^*(x_{*i})}\,. \tag{3.4}$$

Equation (3.4) is exact, irrespective of the analytic structure of z and z^*, since it was derived using only local deformation of contours. The right-hand side is now divided into two parts: the first two terms are nonlocal since they involve an integral on the real axis but for the same reason they have a rather regular behavior when $\mathrm{Im}\, x \neq 0$. In particular, when z (respectively z^*) are finite, the first, (respectively second) integral considered as a function of z, (respectively z^*) can be Taylor expanded in powers of $z - z(x)$ or $z^* - z^*(x)$, which shows that the nonlocal terms cannot be more singular than the spacial derivatives $\partial_x z$ and $\partial_x z^*$. The last two terms in (3.4) are much more surprising since they relate the dynamics at x to the properties of the maps z and z^* at some of his co-preimages. We understand at once that singularities may occur when any of the x_i or x_{*i} gets close to a

zero of $\partial_x z$ or $\partial_x z^*$, which is why "critical" is an apt term for these points.

3.2. First generation singularities

Let us assume that at the initial time the interface is described by some analytic function $z_0(x)$. The map z_0 has a countable set of critical points. Critical points are where a pair of co-preimages merge together. Around such a point, x_0, the Taylor expansion of z_0 starts at quadratic order,

$$z_0(x) - z_0(x_0) \sim \tfrac{1}{2} a (x - x_0)^2 \quad \text{as} \quad x \to x_0 \,. \tag{3.5}$$

We do not expect anything spectacular to happen for $x \sim x_0$ from eq. (3.4). At worst, one of the co-preimages of x crosses the real axis to create a double root with x at x_0, i.e. $x_t(x) \sim 2x_0 - x$, but the local contribution to (3.4) thereby generated reduces to a constant.

A slightly more complicated situation whereby a critical point does induce a singularity in (3.4) is created by letting x approach x_1 where $z_0(x_1) = z_0(x_0)$ and $\partial_x z_0(x_1) \neq 0$. Among the other co-preimages of x there are two x_a, x_b say, which merge when $x = x_1$ and form the double root at x_0. It is at this step that we must assume $z_0(x)$ is at least cubic, and as shown in the appendix a cubic polynomial is sufficient to generate all the complexity which follows.

Assume as $x \to x_1$ from the real axis, one of the x_a, x_b to be called henceforth $\tilde{x}$, crosses the real axis an odd number of times and thereby appears in (3.4). (If both x_a and x_b cross the real axis from the same side there will be two terms in (3.4) which cancel in the limit; but this does not happen for the cubic.) We have therefore created an intrinsic singularity in (3.4) since $\partial_x z(\tilde{x})$ in the denominator tends to zero while the numerator approaches $\partial_x z(x_1) \neq 0$. (Note $\partial_x z(\tilde{x})$ is the x-derivative of z evaluated at $\tilde{x}$; the x dependence of $\tilde{x}$ is immaterial). By retaining just the singular term, the equation of motion simplifies to

$$\partial_t z(x, t) = -\tfrac{1}{2} \mathrm{i} \frac{\partial_x z(x, t)}{\partial_x z(\tilde{x}, t)} = -\tfrac{1}{2} \mathrm{i}\, \partial_x \tilde{x}(x, t) \,, \tag{3.6}$$

where the last equality is a consequence of $z(x, t) = z(\tilde{x}, t)$. The sign we chose in (3.6) is arbitrary and of no importance in the following. The dynamics of z for x near x_1 will turn out to be singular in t at short times ($\sim t^{2/3}$). On the other hand, z for x near x_0 is analytic in t and by comparison slow. Therefore, to a good approximation, we can consider the local expansion of z near $z_0(x_0)$ as being valid at $t > 0$ with x_0 and a in (3.5) unchanged. In this way, we obtain the series of equalities

$$\begin{aligned} \tilde{x} - x_0 &= \sqrt{\frac{2}{a} (z_0(\tilde{x}) - z_0(x_0))} \\ &\approx \sqrt{\frac{2}{a} (z(\tilde{x}, t) - z_0(x_0))} \\ &= \sqrt{\frac{2}{a} (z(x, t) - z_0(x_1))} \,. \end{aligned} \tag{3.7}$$

The last equality allows one to express $\tilde{x}(x, t)$ only in terms of the properties of z for x near x_1 and eq. (3.6) becomes, using (3.7)

$$\partial_t z(x, t) = -\frac{\mathrm{i}}{2\sqrt{2a}} \frac{\partial_x z(x, t)}{\sqrt{z(x, t) - z_0(x_1)}} \,. \tag{3.8}$$

This Burgers-like equation is easily solved, using the Hodograph method [7]. Looking for x as a function of z and t, one can rewrite (3.8) as

$$\partial_t x(z, t) = \frac{\mathrm{i}}{2\sqrt{2a}} \frac{1}{\sqrt{z - z_0(x_1)}} \,, \tag{3.9}$$

whose solution has the general form

$$x - x_1 = \frac{\mathrm{i}}{2\sqrt{2a}} \frac{t}{\sqrt{z - z_0(x_1)}} + F(x) \,, \tag{3.10}$$

where $F(z)$ is entirely specified by the initial conditions. Since x_1 is a regular point of the map z at the initial time, in its neighborhood one has

$z_0(x) - z_0(x_1) \sim b_1(x - x_1)$ where $b_1 = \partial_x z_0(x_1)$, so that our final result is

$$x - x_1 = \frac{\mathrm{i}}{2\sqrt{2a}} \frac{t}{\sqrt{z - z_0(x_1)}} + \frac{z - z_0(x_1)}{b_1} . \tag{3.11}$$

Note immediately that for $t > 0$, x_0 no longer has a co-preimage in the neighborhood of x_1 and in this sense the singularity in (3.4) has been regularized.

To examine the local structure of z for x near x_1 at short times, eq. (3.11), which is a third-order polynomial in $h = \sqrt{z - z_0(x_1)}$, can be inverted explicitly. The three roots $h_k(x - x_1, t)$, $0 \leq k \leq 2$, are nothing but the same analytic function extended on three Riemann sheets [8]. We write them below in a way which makes their asymptotic properties at infinity evident

$$h_k(x - x_1, t) = \frac{\mathrm{i}}{\sqrt{3}} \sqrt{b_1(x - x_1)} \left(\beta_k U - \frac{1}{\beta_k U} \right)$$
$$= \tfrac{1}{2}\mathrm{i} \left(\frac{b_1^2}{-2a} \right)^{1/6} \sqrt{X}\, t^{1/3} \left(\beta_k U - \frac{1}{\beta_k U} \right) , \tag{3.12a}$$

with

$$\beta_k = \mathrm{e}^{2\mathrm{i}k\pi/3} \tag{3.12b}$$

$$U = \mathrm{e}^{-2\mathrm{i}\pi/3} \left(\sqrt{1 - \frac{1}{X^3}} - \frac{\mathrm{i}}{X^{3/2}} \right)^{1/3} , \tag{3.12c}$$

$$X = \frac{x - x_1}{v_1} , \quad v_1 = \tfrac{3}{2} \frac{t^{2/3}}{(-4ab_1)^{1/3}} . \tag{3.12d}$$

The most important thing to notice in (3.12c) is the emergence of square root singularities at $X^3 = 1$, i.e. at three points $x - x_1 = v_1 \mathrm{e}^{2\mathrm{i}k\pi/3}$ which move away from x_1 as $t^{2/3}$. Let us make clear how the various algebraic quantities entering (3.12a) are defined: we put three branch cuts between x_1 and $x_1 + \beta_k v_1$. If x_1 lies in the lower complex half plane, we single out from these three branch cuts, one pointing in the direction of negative imaginary parts and extend it to infinity (see fig. 2). Then the phase of X is measured with respect to this direction, so that the phase of $\sqrt{X}$ in front of the brackets in (3.12a) varies from 0 to π during an anticlockwise 2π turn around x_1 and $1/X^{3/2}$ inside U from 0 to -3π. On the other hand we take the argument of $1 - 1/X^3$ between $-\pi$ and π. For $|X| \gg 1$, the argument is zero. For $|X| < 1$, the argument of $1 - 1/X^3$ varies from $+\pi$ to $-\pi$ when one goes in an anticlockwise way from one branch to the other and it suffers a 2π jump at each branch. The argument of $\sqrt{1 - 1/X^3}$ is just the half of this quantity.

With such conventions, it can be checked that the first root h_0 is indeed the solution on the physical sheet, for points approaching x_1 from the real axis without encircling any singularity (see fig. 2). We recover, as required, $h_0(x - x_1) \sim \sqrt{b_1(x - x_1)}$ for $|X| \gg 1$. The second root, h_1, gives the solution on the second Riemann sheet and from (3.12a)–(3.12c) vanishes for $|X| \gg 1$. On the third Riemann sheet h_2 behaves asymptotically like $-h_0$. In fig. 3, we show how the roots are permuted when one crosses the three branch cuts emanating from x_1.

To get more insight into this analytic structure, it is useful to ask how many new co-preimages

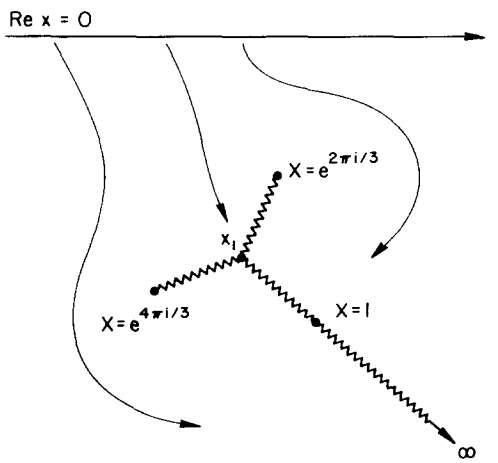

Fig. 2. The physical Riemann sheet around x_1 at $t > 0$: wiggly lines indicate the branch cuts described in the text, lines with arrows are the paths of analytic continuation from the real axis leading to the root h_0.

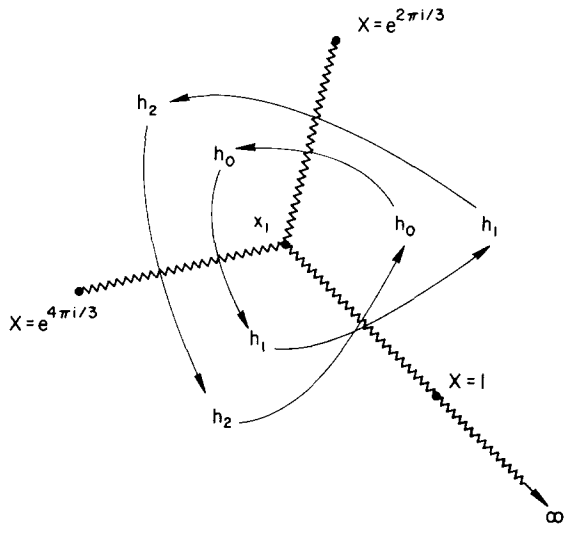

Fig. 3. The permutation of roots h_0, h_1, h_2 as x moves around x_1 through branch cuts.

each point x has acquired and where they lie as x explores the complex plane. We simply get the answer by coming back to eq. (3.11): the inverse square root at $z = z_0(x_1)$ tells us that any value of z is now the image of two different values of x, which means the creation of one new co-preimage for any x. For x far from x_1 (i.e. $X \gg 1$ in (3.12a) or $t \to 0$ in (3.11)), the new co-preimage is located in the third Riemann sheet ($h_2 \sim -h_0$ for $X \gg 1$). It enters the second Riemann sheet when x approaches x_1; in particular the value $z(x_0)$ which equaled $z(x_1)$ at $t = 0$ is now assumed at x equals infinity in the second Riemann sheet ($h_1 \to 0$ as $|X| \to +\infty$). This closes our discussion of the content of eqs. (3.11) and (3.12a). It should be mentioned that the above analysis breaks down at a distance of order $\mathcal{O}(t)$ from x_1. The actual motion of x_0 (analytic in t) complicates the actual structure, very close to x_1. Our analysis correctly captures the outer $\mathcal{O}(t^{2/3})$ region, which will only matter in the following.

Before pursuing how other critical points can nucleate additional singularities on top of those just found, we pause to consider the motion of the square root singularities just found. If they have no preimage under z or z^* which is singular or a critical point, then (3.4) implies an equation of the form

$$\partial_t z = A\, \partial_x z - A^*\, \partial_x z^* + B\,,$$

where A, A^* and B are smooth. Therefore, for short enough times the square root singularities are simply advected. If they reach the real axis, physical singularities will appear which are stronger than those associated with Kelvin–Helmholtz rollup.

We now ask whether new critical points have been generated as a result of solving (3.8). Rewriting (3.1) as

$$h^3 - b_1(x - x_1)h + \frac{\mathrm{i}t b_1}{2\sqrt{2a}} = 0 \tag{3.13}$$

and differentiating with respect to x, we get

$$\partial_x z = 2h\, \partial_x h = \frac{2b_1 h^2}{3h^2 - b_1(x - x_1)}\,. \tag{3.14}$$

Since h never vanishes except at x equals infinity, neither does $\partial_x z$. This clearly eliminates the possibility that new critical points of z are generated within the regime of validity of (3.11), (3.12a) but this is emphatically not true for the map z^* which enters (3.4) on equal footing with z. Indeed, from the definitions of z and z^*, it follows that critical points of z^* are points where $\partial_x z = 2$, a condition which is met whenever

$$z - z_0(x_1) = h^2 = \frac{b_1}{3 - b_1}\,(x - x_1) \tag{3.15}$$

according to (3.14). Inserting (3.15) into (3.13) allows one to solve easily for $x - x_1$,

$$x - x_1 = \frac{1 - \frac{1}{3}b_1}{(1 - \frac{1}{2}b_1)^{2/3}}\, v_1 \beta_i\,, \tag{3.16}$$

with $v_1 \sim t^{2/3}$ given in (3.12d), and $\beta_i^3 = 1$.

Provided b_1 is not too close to 2, the three points we find lie close to x_1 within the range of validity of our local analysis. Remember that

$b_1 = \partial_x z_0(x_1) = 2$ would correspond to x_1 being a critical point of z^* at the initial time, a highly nongeneric situation. We should say that even with an explicit result for the positions of these new critical points of z^*, it is much more difficult to ascertain on which Riemann sheet each of these points resides. We shall not attempt to answer this question here because it does not affect the ability of these new critical points to act as sources of a second generation of singularities, (as we shall see in the next section the only thing we need is the existence of a path leading from the real axis to these points). However, this issue is clearly important in understanding whether, at later times, these new critical points can eventually get close to the real axis and be observed as new folds of the interface. But this difficult problem is beyond the scope of the present work.

Let us summarize what has been done until now: a critical point of the map z at time $t = 0$ (e.g. x_0), emits at time $t > 0$ a self-similar structure of the form $z(x, t) - z(x_1, t = 0) = t^{2/3} Z((x - x_1)/t^{2/3})$ in the vicinity of its co-preimage x_1 at $t = 0$. In the process, the co-preimage itself is destroyed and square root singularities in z are formed. We have found that this self-similar structure contains also new critical points of z^* and we are now in position of repeating the same analysis utilizing these new points. This, we do in the next section.

3.3. Second generation of singularities

The second generation of singularities is slightly different from the first one since the input in this problem is the self-similar structure obtained in the last subsection, to be contrasted with the almost time-independent input (3.5) used for the first generation. That is why this question deserves some attention. Furthermore, the analysis we shall present here can readily be extended to subsequent generations which do not raise any new difficulty.

To be able to derive an equation equivalent to (3.7) in the last subsection, we first need to know the inverse map $x(z^*, t)$ for z^* near $z_0^*(x_1)$ and x near x_1. The subscript $*$ on x that was employed in subsection 3.1 to distinguish inverses under z and z^* will be omitted in this subsection because only z^* is pertinent. A nice algebraic expression can still be derived at the second-generation level. Inserting

$$z(x, t) - z_0(x_1) = 2(x - x_1) - (z^*(x, t) - z_0^*(x_1)) \tag{3.17}$$

into (3.11), one gets

$$\left(x - x_1 + \frac{z^* - z_0^*(x_1)}{b_1 - 2}\right)^2 \times \left(x - x_1 - \frac{z^* - z_0^*(x_1)}{2}\right) + \left(\frac{b_1}{b_1 - 2}\right)^2 \frac{t^2}{16a} = 0 . \tag{3.18}$$

The three roots of the third-order polynomial in $(x - x_1)$ are given by

$$x - x_1 = f_k(z^* - z_0^*(x_1), t) = \frac{z^* - z_0^*(x_1)}{6(b_1 - 2)} \left[b_1 - 6 + b_1\left(\beta_k V + \frac{1}{\beta_k V}\right)\right], \tag{3.19}$$

where $\beta_k = e^{2ik\pi/3}$, $0 \le k \le 2$, is a cube root of unity and

$$V = \left(1 - \frac{2}{Y^3} + 2i\sqrt{\frac{1}{Y^3}\left(1 - \frac{1}{Y^3}\right)}\right)^{1/3}, \tag{3.20a}$$

$$Y = \frac{z^* - z_0^*(x_1)}{\gamma_1 t^{2/3}}, \quad \gamma_1 = \tfrac{3}{2}\left(\frac{b_1 - 2}{b_1 a}\right)^{1/3}. \tag{3.20b}$$

Therefore any value z^* near $z_0^*(x_1)$ has three preimages near (x_1) in contrast to z which has only two. Both roots $k = 1, 2$ have the same asymptotic behavior $x - x_1 \sim -[z^* - z_0^*(x_1)]/(b_1 - 2)$ for $|Y| \gg 1$ and it is not easy to decide which one describes the solution on the physical Riemann sheet. Only a careful comparison of

(3.19) with (3.12a) could help to settle this point but which we will not attempt in this work.

The square root singularities in (3.19) at $Y^3 = 1$ signal the critical points of z^* in the neighborhood of x_1 at $t > 0$ which were found before. The various quantities in (3.19) and (3.20) are defined as follows: we put three branch cuts between $Y = 0$ and $Y = e^{2ik\pi/3}$, $0 \leq k \leq 2$. The phase of $1 - 1/Y^3$ is chosen between $-\pi$ and $+\pi$, where both limiting values are reached, respectively, on the right- and left-hand sides (as seen from the origin) of the three branch cuts. In the same way we ascribe to the argument of the cube root in the definition of V, a phase between $-\pi$ and π (again these limiting values are reached only on the branch cuts). Finally we note that a $\frac{2}{3}\pi$ turn changes the quantity $1/Y^{3/2}$ inside of the cube root in V into its opposite and as a consequence V into $1/V$. Therefore, neighboring branch cuts are not equivalent but the symmetry is restored by a $\frac{4}{3}\pi$ rotation. The two-fold indeterminacy on the sign of $1/Y^{3/2}$ is related to the choice of the right solution on the physical space been h_1 and h_2. As discussed before, we must leave this issue open. Figure 4 indicates some possible permutations of roots deduced from (3.19) as branch cuts are crossed. Using the rules defined above, it can also be checked that at each point $Y = e^{2i\pi k/3}$ (or $z_1^{*k}(t) - z_0^*(x_1) = \gamma_1 t^{2/3} e^{2i\pi k/3}$) only two of the three roots f_k are singular. From (3.19) and (20), the amplitudes of the square root singularities

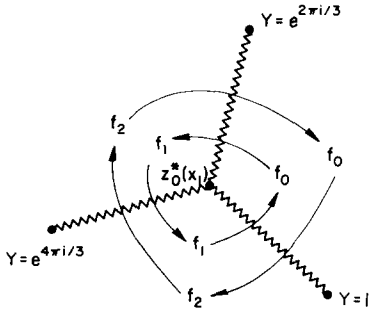

Fig. 4. Some permutations of the roots f_i as X^* moves around $z_0^*(x_i)$ through the branch cuts.

are found to be equal to

$$x - x_1 \sim \alpha_1^k [z^* - z_1^{*k}(t)]^{1/2}, \tag{3.21a}$$

$$\alpha_1^k = \pm \frac{b_1 t^{1/3}}{3(b_1 - 2)} e^{i\pi k/3} \sqrt{\gamma_1}. \tag{3.21b}$$

They are smaller by a $t^{1/3}$ factor than the amplitude of the square root singularities $\sqrt{2/a}$, we started from in the first generation problem, (cf. (3.5)).

Having clarified the analytic structure of the inverse map $x(z^*, t)$ near $z_0^*(x_1)$, we are now in position of asking how it may affect z^* for x in the neighborhood of co-preimages of x_1 as the time evolves. Let x_2 be a co-preimage of (x_1) under the map z^* at $t = 0$ (i.e. $z_0^*(x_2) = z_0^*(x_1)$). As x approaches x_2 from the real axis, only one of its co-preimages, to be called henceforth $\tilde{x}$, goes to x_1 at the initial time, since x_1 is unlikely to be also a critical point of z_0^*. (For $t > 0$ this means that in the neighborhood of x_1 there is an x obtained from (3.19) for $z^* = z_1^{*k}(t)$ (defined above (3.21)) where $\partial_x z^* = 0$.) Assume again that this co-preimage crosses the real axis an odd number of times during the analytic continuation towards x_2. By continuity, this property still holds at short positive times. We know that other co-preimages of x appear near (x_1) at $t > 0$ but they reside on other Riemann sheets and are not able to cross the real axis of the physical sheet. Therefore, according to the dynamical rules established in subsection 3.1, they cannot intervene in the r.h.s. of eq. (3.4). Repeating the arguments of the last subsection which led to (3.8) via (3.6) and (3.7) (we promote x_1 to x_2, x_0 to x_1 and z to z^*) we find $\tilde{x}$ induces a singular contribution in the equation of motion for x near (x_2) of the form

$$\partial_t z^* = -\tfrac{1}{2} i \partial_x z^* f'(z^*(x, t) - z_0^*(x_2), t), \tag{3.22}$$

where f' is the derivative with respect to z^* of the function f defined in (3.19) and the sign of the r.h.s. has been chosen arbitrarily. Note that

diverges at $Y^3 = 1$. This constitutes an alternative scenario through which divergences in the equation of motion (3.4) originating from the existence of critical points of z or z^* are regularized. Since these new critical points of z^* near x_2 belong to the same preimage as their parents near x_1 of the first generation, it is not completely obvious that they may generically induce themselves new daughter singularities of z^*.

Instead, to pass onto the third generation singularities we revert to critical points of z. Using the fact that $\partial_x z = 0$ is equivalent to $\partial_{z^*} x = \frac{1}{2}$, one deduces from (3.25) that this last condition is met for

$$z^* = z_2^{*k}(t) = \tilde{z}_2^{*k}(t) + \left(\frac{2b_2}{b_2 - 2}\,\tilde{\alpha}_2^k\right)^2 . \qquad (3.28)$$

Thus, each critical point of z^* near (x_1) that appeared after solving the first generation problem gives rise to a single new critical point of z near (x_2) for the second generation. Whereas in (3.28) $\tilde{z}_2^{*k}(t)$ is not known to better than a $t^{2/3}$ accuracy since we have neglected from the beginning regular terms in the r.h.s. of (3.22) which yield corrections of order t, the $t^{4/3}$ scaling of the relative position $z_2^{*k}(t) - \tilde{z}_2^{*k}(t)$ is meaningful. To leading order in $t^{2/3}$, the location of these new critical points in the z plane follows from $z = 2x - z^*$ with x from (3.26):

$$z_2^k(t) = z_0(x_2) + \frac{2 - b_2}{b_2}\,\gamma_1 t^{2/3}\,\mathrm{e}^{\mathrm{i}2\pi k/3} . \qquad (3.29)$$

By definition the inverse map $x(z)$ near $(x_2, z_0(x_2))$ must display square root singularities for $z = z_2^k(t)$. To compute the amplitude of these square root singularities, denoted α_2^k, one could, in the spirit of what we did at the beginning of this subsection, derive a local expression of $x(z)$ from the inverse map $x(z^*)$ which was obtained (3.26). They can also be obtained from the definition: $\alpha_2^k = \sqrt{2}(\partial^2 z/\partial x^2)^{-1/2}(x(z_2^{*k}(t)))$ and use the set of equalities:

$$(\partial^2 z/\partial x^2)(x(z_2^{*k}(t))) = -(\partial^2 z^*/\partial x^2)(x(z_2^{*k}(t)))$$
$$= \frac{(\partial^2 x/\partial z^{*2})(z_2^{*k}(t))}{(\partial x/\partial z^*)^3(z_2^{*k}(t))} = 8(\partial^2 x/\partial z^{*2})(z_2^{*k}(t)) . \qquad (3.30)$$

The last quantity in (3.30) is easily deduced from (3.27) and (3.28) and leads to amplitudes henceforth called α_2^k, which together with $\tilde{\alpha}_2^k$, scale as $t^{2/3}$.

The third- (or higher-) order generation can be studied by following exactly the pattern we have followed for the second-order generation. Considering x_3 a co-preimage of x_2 under z at time $t = 0$ and assuming it to be under the influence of the critical point near x_2 (in the sense defined by $\partial_x z(x_2 + \mathcal{O}(t^{2/3})) = 0$ we shall obtain an equation analogous to (3.22) with z^* replaced by z and x_2 by x_3. A natural generalization of (3.27) allows us to calculate from $z_2^k(t)$ and α_2^k, the leading order position and amplitude $\tilde{z}_3^k(t)$, $\tilde{\alpha}_3^k$ of the square root singularities appearing at $t > 0$ in $x(z, t)$ near $(x_3, z_0(x_3))$. We have then shown how to relate by simple algebraic manipulations the singularities of $x(z, t)$ to the ones of $x(z^*, t)$ (eqn. (3.28)–(3.30)). Clearly, the procedure can be carried out further since to study the $(n+1)$th step, one needs from the solution at the nth step only the position of the square singularity to order $t^{2/3}$ and their amplitudes α_n^k to leading order in t ($\sim t^{n/3}$).

It remains to see whether there exist initial conditions for which infinitely many singularities are produced by the mechanism discussed in this section. As shown in the appendix, the answer is yes for such a simple initial curve as a cubic.

4. Conclusion

We began by noting that the numerical solution of (1.1), (1.2) revealed a significantly more subtle blow up problem than has previously been encountered. There is no self-similar scaling form within which all time dependence dis-

appears and no way to reduce the dimension of the problem.

The interface equation for this problem, (1.3), is very reminiscent of the Birkhoff–Root equation for a vortex sheet. We found it useful to parametrize the complex interface position, z, in eq. (1.3) in terms of the variable x instead of the Lagrangian variable γ, thus leading to eqs. (2.4) and (2.7). This is acceptable if no overhang develops which was found to be the case in the numerical solutions of (1.1) and (1.2).

As a first approximation to this problem, we have carried over for our parametrization the simplifications which, for the Birkhoff–Rott equation, provided a consistent solution to the Kelvin–Helmholtz roll-up problem. The resulting equations are the least severe approximation to (2.4), (2.7) which we can imagine, and were shown in section 2 to be completely inadequate. They failed to give any finite-time singularities for meromorphic initial conditions.

There are several caveats concerning the fidelity of our approximation to ref. [4]. Firstly, ref. [4] expands in the Lagrangian parameter γ, as is natural when the circulation is conserved. For our problem this approximation was intractable though we could of course revert to a γ parametrization once we have solved with x as a parameter. Also, ref. [4] assumed complex square root singularities in their initial data and then proved that they propagated intact and classified the singularity they induced upon reaching the real axis. We have only treated meromorphic initial data for (2.7) and have not examined how weaker singularities propagate.

Physically, one may ask if the curvature singularity indicative of a roll-up is present in (1.3). We are inclined to say no since it did not seem to develop in the numerical solutions of the continuum equations (1.1), (1.2), even when the interface was thin and inclined at an appreciable angle to $\hat{x}$. In addition, the Kelvin–Helmholtz instability is inertial and not expected for porous media flow while it is present in two-dimensional Boussinesq convection. One might object that the order of the equations with respect to $\mathrm{d}/\mathrm{d}t$ so obvious in the continuum limit, (i.e. in (1.2), velocity, and not acceleration equals force) is obscured in (1.3) since if the numerator is replaced by a constant, the Birkhoff–Rott equation results. We believe this is a dangerous replacement when the curvature diverges but we have no quantitative argument. We do insist that for a singularity of (1.3) to be relevant to (1.1), (1.2) $|\partial_\gamma z|^{-1}$ must go to zero since this scales with the interface thickness by area preservation.

In section 3, we showed how for short times, complicated branching structure develops in the complex x-plane for $z(x)$ when (1.3) is solved more exactly. We believe these singularities are correct for the exact solution to (1.3) for initial condition near to a cubic. That being said, we have no idea whether the same mechanism operates for more general initial conditions, and whether for longer times what we have found would reach the real x-axis and become a physical singularity.

Acknowledgement

This research was supported by the Air Force Office of Scientific Research grant # No. 91-0011.

Appendix

We investigate in this appendix the geometry of preimages in the case of a cubic curve. We show that such initial conditions can give rise to an infinite sequence of singularities, by the mechanism discussed in section 3 of this paper. This possibility is found to depend on the value of the slope of the profile at the origin.

Without loss of generality, we write the cubic in the canonical form,

$$y = \tfrac{1}{6}x^3 + cx\,. \tag{A.1}$$

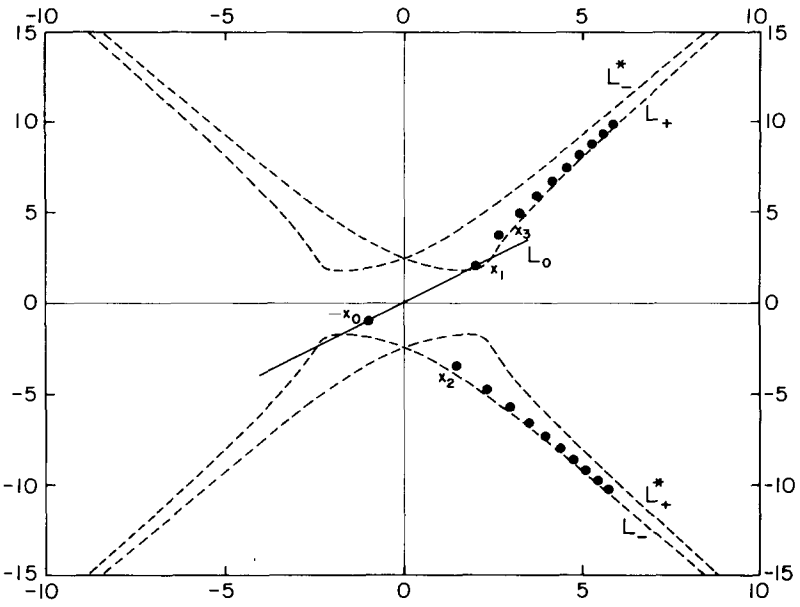

Fig. 5. The complex x-plane showing the critical point $-x_0$ and its co-preimages $x_1, x_2, \ldots$ (solid circles) under z and z^* as explained in the text for $z(x) = x + \frac{1}{6}ix^3$. Dotted lines represent the curves $L_\pm$, $L_\pm^*$ defined in the text. Solid circles are the iterate points x_m, $0 \le n \le 20$ constructed from $-x_0$ according to the rules given in the text.

The co-preimages of x under the map z are solutions of

$$x + i(\tfrac{1}{6}x^3 + cx) = x' + i(\tfrac{1}{6}x'^3 + cx') . \qquad (A.2)$$

Besides x, this equation has two roots

$$x_\pm = -\tfrac{1}{2}x \pm i\tfrac{1}{2}\sqrt{3}\sqrt{x^2 - 4x_0^2} , \qquad (A.3)$$

where $x_0 = \sqrt{2(i - c)}$ and $-x_0$ are the two critical points of the map z. For x on the real axis, (A.3) defines two curves in the upper and lower half complex planes, to be called henceforth L_+ and L_- which are drawn in fig. 5 for $c = 0$. We note that at large $|x|$, $\mathrm{Arg}\, x_\pm \sim \frac{1}{3}\pi(\frac{2}{3}\pi)$. The straight line joining the origin to $\pm x_0$ plays an important role in the following discussion and we shall call it L_0. L_0 crosses $L_\pm$ at the points $\pm\sqrt{3}x_0$ which are nothing but the co-preimages of 0. From (A.3), it is obvious that a point x on L_0 between $-2x_0$ and $2x_0$ has its two co-preimages on the same segment, a property which will be used later.

Similarly, the co-preimages of x under the map z^* are given by

$$x_\pm = -\tfrac{1}{2}x \pm i\tfrac{1}{2}\sqrt{3}\sqrt{x^2 - 4x_0^{*2}} . \qquad (A.4)$$

This defines two curves L_+^* and L_-^*, respectively in the lower and upper half complex planes, which are complex conjugates of L_+ and L_-. L_+^* and L_- (respectively L_-^* and L_+) are asymptotic to each other at infinity. The counterpart of L_0, L_0^* can also be introduced, with the same properties as L_0 with respect to z^*.

Let Ω denote the region in the complex plane between L_- and L_+. Useful insight into the geometry of preimages is provided by the following lemma:

Lemma. The preimages of any value of z consist of one point $w_1(z)$ outside Ω and two others $w_2(z)$ and $w_3(z)$ inside Ω. If $\mathrm{Im}\, w_1 \ge 0$ (respectively ≤ 0), then $\mathrm{Im}\, w_2$, $\mathrm{Im}\, w_3 \le 0$ (respectively ≥ 0), and w_2, w_3 lie on opposite sides of L_0. A similar result holds for z^*.

To prove the lemma, we first establish the existence of at least one preimage outside Ω. Let w_2 be a preimage inside Ω (if there is no such w_2 we need not go further) and assume without loss of generality w_2 has a negative imaginary part. Let now x approach w_2 from $-x_0$ so as not to cross L_- or the real axis. When $x = -x_0$ the two co-preimages x_-, x_+ are respectively at $-x_0$ and $+2\,x_0$. Therefore one of the points is inside Ω, the other one outside (fig. 6). This property is conserved as x moves from $-x_0$ to w_2 on the path described before, because x_+, x_- are forbidden to cross L_+ or L_-. (Simultaneously x_- goes to w_3 and x_+ goes to w_1.)

We want to show now that w_1 is unique and check the other assertions of the lemma: assume again without loss of generality w_1 has a positive imaginary part. We let x approach w_1 by first going from 0 to $2\,x_0$ and then from $2\,x_0$ to w_1. In the particular case where w_1 lies on L_0 between $\sqrt{3}x_0$ and $2\,x_0$, the path is stopped at w_1, before reaching $2\,x_0$ and we know that w_2 and w_3 are on

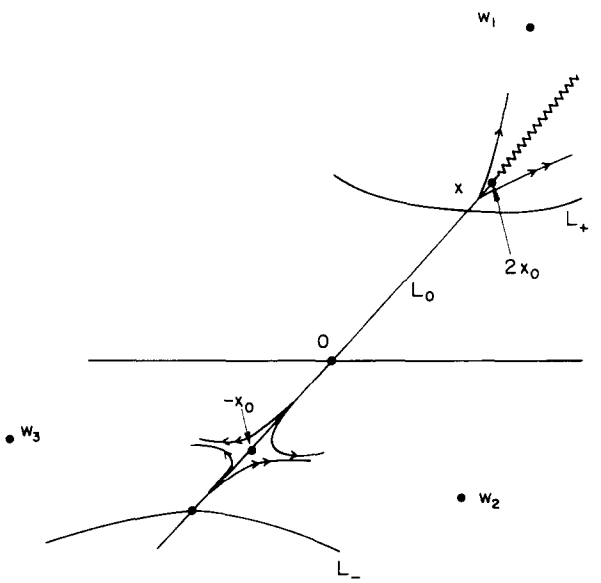

Fig. 6. The geometry of the complex x-plane used to establish the lemma. The lines with one (respectively two) arrows show how the three preimages of a given z move in the vicinity of the critical point, $-x_0$ and its co-preimages $2x_0$, and tend towards w_j. The lines $L_{+,-,0}$ are unchanged from fig. 5. The wiggly line is the branch cut of eq. (A.3).

L_0 between 0 and $-\sqrt{3}x_0$, thereby satisfying the lemma. In the general case, when x passes by $2\,x_0$, its preimages $\tilde{x}_+$ and $\tilde{x}_-$ get close to $-x_0$ and follow the trajectories depicted in fig. 6. Figure 6 is understood analytically by expanding (A.3) for x near $2\,x_0$. If $x = 2\,x_0\,(1+\epsilon)$ with $\epsilon \ll 1$ and $0 \leq \mathrm{Arg}\,\epsilon < 2\pi$, one finds indeed

$$\tilde{x}_\pm \sim -x_0(1 \mp \sqrt{6e^{-i\pi}\epsilon})\,. \tag{A.5}$$

If x remains outside Ω while completing the last part of its path from $2x_0$ to w_1, $\tilde{x}_+$ and $\tilde{x}_-$ remain in Ω. Otherwise x would cross L_+. For the same reason, $\tilde{x}_+$ and $\tilde{x}_-$ never cross again the real axis, which proves $\mathrm{Im}\,w_2$, $\mathrm{Im}\,w_3 \leq 0$. Neither do they cross L_0 because x would then be on L_0 between $\sqrt{3}x_0$ and $2\,x_0$, something we excluded from the beginning. Therefore w_2 and w_3 lie on opposite sides of L_0, as announced.

We are now able to give a geometric criterion for the production of new singularities: suppose that at the nth step new critical points of z have been generated near x_n. The following iterate point must be chosen among the two co-preimages of x_n for the map z. Daughter singularities may appear near x_{n+1}, if and only if as x approaches x_{n+1} from the real axis, one of its two co-preimages goes to x_n after crossing the real axis once. In other words x_{n+1} must be outside Ω, with $x_+(x_{n+1}) = x_n$ for $\mathrm{Im}\,x_{n+1} > 0$ or $x_-(x_{n+1}) = x_n$ for $\mathrm{Im}\,x_{n+1} < 0$. By the preceding lemma, x_{n+1} outside Ω means x_n inside Ω, while the same condition applied to the nth step requires x_n outside Ω^*. The resulting constraint on the position of x_n is rather severe in the case of the cubic since Ω and the complement of Ω^* do not have a large intersection. On the other hand, the condition that $x_+(x_{n+1}) = x_n$ for instance when $\mathrm{Im}\,x_{n+1} > 0$, is not restrictive: it just defines how the path to x_{n+1} should encircle $2x_0$, as is obvious from fig. 6 or directly from (A.3). At the next step, the roles of the maps z and z^* are interchanged and the condition for x_{n+1} is that it belongs to Ω^* but not to Ω.

In fig. 5 we have plotted the first twenty iterate points x_n with the initial point $-x_0$ and a zero value of the slope at the origin. We observe that the criterion is obeyed up to $n = 20$ (it is so even up to $n = 40$). Although we lack a mathematical proof of the result, the figure suggests that the cascade does not end in this case with, asymptotically, iterate points slowly drifting just above L_+ or L_-. However, this property seems to hold only in a narrow range of values of c around $c = 0$. For negative values of c, the series of iterate points tends to get below L_+ and L_-: we found for instance that the cascade breaks at the fourth iterate when $c = -0.5$. For positive values of c, the trend is opposite: the series of iterate points gets progressively closer to the upper boundaries L_-^* and L_+^* and the cascade ceases to exist in any case for $c \geq 3$.

References

[1] D. Bensimon et al., Rev. Mod. Phys. 58 (1986) 977; S.D. Howison, Europ J. Appl. Math., submitted.

[2] G. Trygvasson and H. Aref, J. Fluid Mech. 136 (1983) 1.

[3] A. Pumir and E. Siggia, unpublished.

[4] R. Caflisch and S. Semmes, Physica D 41 (1990) 197; R. Caflisch, N. Ercolani and T. Hou, preprint (1991).

[5] B. Shraiman and D. Bensimon, Phys. Rev. A 30 (1984) 2840;
S.D. Howison, Proc. R. Soc. Edin. A 102 (1985) 141; S.D. Howison, J. Fluid Mech. 167 (1986) 439.

[6] D.W. Moore, Proc. R. Soc. London A 365 (1979) 105; R. Caflisch, O. Orellana and M. Siegel, SIAM J. Appl. Math. 50 (1990) 1517.

[7] R. Courant and D. Hilbert, in: Methods of Mathematical Physics, Vol. II (Interscience, New York, 1962).

[8] E. Hille, in: Analytic Function Theory, Vol. II (Ginn and Co., New York, 1962).